PAPER

Kinetic modelling of runaway electron avalanches in tokamak plasmas

To cite this article: E Nilsson *et al* 2015 *Plasma Phys. Control. Fusion* **57** 095006

IOP Publishing Plasma Physics and Controlled Fusion

Plasma Phys. Control. Fusion **57** (2015) 095006 (11pp) doi:10.1088/0741-3335/57/9/095006

Kinetic modelling of runaway electron avalanches in tokamak plasmas

E Nilsson[1], J Decker[2], Y Peysson[1], R S Granetz[3], F Saint-Laurent[1] and M Vlainic[4,5]

[1] CEA, IRFM, F-13108 Saint-Paul-lez-Durance, France
[2] Ecole Polytechnique Fédérale de Lausanne (EPFL), Centre de Recherches en Physique des Plasmas (CRPP), CH-1015 Lausanne, Switzerland
[3] MIT Plasma Science and Fusion Center, Cambridge, MA 02139, USA
[4] Department of Applied Physics, Ghent University, B-9000 Ghent, Belgium
[5] Institute of Plasma Physics AS CR, 18200 Prague, Czech Republic

E-mail: emelie.nilsson@cea.fr

Received 13 March 2015, revised 8 June 2015
Accepted for publication 7 July 2015
Published 30 July 2015

Abstract

Runaway electrons can be generated in tokamak plasmas if the accelerating force from the toroidal electric field exceeds the collisional drag force owing to Coulomb collisions with the background plasma. In ITER, disruptions are expected to generate runaway electrons mainly through knock-on collisions (Hender *et al* 2007 *Nucl. Fusion* **47** S128–202), where enough momentum can be transferred from existing runaways to slow electrons to transport the latter beyond a critical momentum, setting off an avalanche of runaway electrons. Since knock-on runaways are usually scattered off with a significant perpendicular component of the momentum with respect to the local magnetic field direction, these particles are highly magnetized. Consequently, the momentum dynamics require a full 3D kinetic description, since these electrons are highly sensitive to the magnetic non-uniformity of a toroidal configuration. For this purpose, a bounce-averaged knock-on source term is derived. The generation of runaway electrons from the combined effect of Dreicer mechanism and knock-on collision process is studied with the code LUKE, a solver of the 3D linearized bounce-averaged relativistic electron Fokker–Planck equation (Decker and Peysson 2004 DKE: a fast numerical solver for the 3D drift kinetic equation *Report* EUR-CEA-FC-1736, Euratom-CEA), through the calculation of the response of the electron distribution function to a constant parallel electric field. The model, which has been successfully benchmarked against the standard Dreicer runaway theory now describes the runaway generation by knock-on collisions as proposed by Rosenbluth (Rosenbluth and Putvinski 1997 *Nucl. Fusion* **37** 1355–62). This paper shows that the avalanche effect can be important even in non-disruptive scenarios. Runaway formation through knock-on collisions is found to be strongly reduced when taking place off the magnetic axis, since trapped electrons can not contribute to the runaway electron population. Finally, the relative importance of the avalanche mechanism is investigated as a function of the key parameters for runaway electron formation, namely the plasma temperature and the electric field strength. In agreement with theoretical predictions, the LUKE simulations show that in low temperature and electric field the knock-on collisions becomes the dominant source of runaway electrons and can play a significant role for runaway electron generation, including in non-disruptive tokamak scenarios.

Keywords: plasma physics, runaway electrons, knock-on collisions, tokamak, Fokker–Planck, runaway avalanches

(Some figures may appear in colour only in the online journal)

1. Introduction

Runaway electrons have been observed in magnetic confinement fusion experiments during tokamak operation [1, 4]. They are also encountered in nature in solar flares and electric discharges associated with thunderstorms [5]. Collisional friction forces acting on the electrons reach a global maximum at the thermal velocity (v_{th}) and decrease for higher velocities. In the presence of a strong toroidal electric field (E) collisional drag may consequently be too weak to counteract the acceleration of electrons, which results in continuously accelerated electrons, known as runaway electrons. If no other loss mechanisms than the collisional drag are present [6], runaway electrons may be generated if the electric field exceeds the critical field [7]

$$E_{\mathrm{c}} = \frac{n_{\mathrm{e}} e^3 \ln \Lambda}{4\pi\varepsilon_0^2 m_0 c^2}, \tag{1}$$

where n_{e} is the electron density, m_0 is the electron rest mass, c is the speed of light, e is the elementary charge, and $\ln \Lambda$ is the Coulomb logarithm. The acceleration by a DC field of electrons that diffuse via small angle collisions beyond the critical momentum (p_{c}), defined as the minimum momentum for which collisions are too weak to prevent acceleration of the electrons by the electric field to even higher energies, is referred to as the Dreicer mechanism [7]. In addition, these relativistic electrons can undergo close collisions with bulk electrons and transfer part of their momentum so that also the target electrons may get kicked into the runaway momentum region, while the momentum of the primary electrons remains above the critical momentum. These knock-on collisions lead to multiplication of the number of runaway electrons, commonly referred to as runaway avalanche [3].

Various methods to mitigate the formation of runaway electrons in tokamak plasmas are based on either increasing the plasma density and thereby E_{c} by so-called massive gas injection (MGI) [8], or on deconfining the runaway electrons before they can reach too high an energy, by the means of resonant magnetic perturbations (RMP) [9]. Even though such mitigation methods have been demonstrated in present tokamak experiments, they might not provide a solution for runaways during disruptions in large tokamaks like ITER [10]. Therefore the formation of the runaway electron population is a topic in urgent need of investigation.

Disruptions are interesting but complex processes for studying the birth of runaway electrons, since they include magnetohydrodynamic (MHD) instabilities, anomalous transport and complex evolution of the magnetic field topology [11]. However, the generation of runaway electrons does not necessarily require the extreme conditions found in disruptions. In low density plasmas, the electric field can exceed the critical electric field also during the current flattop in a quiescent plasma [12], free of equilibrium transients, or during current ramp up or ramp down. An advantage of studying runaway formation in these so called non-disruptive scenarios is that the key parameters for the runaway electron mechanisms, mainly the electric field strength, electron density and temperature, can be better diagnosed than during disruptions. Runaway electrons have been detected in non-disruptive scenarios in several of the existing tokamaks [12, 13]. In this work the formation of runaway electrons generated from the combined effect of Dreicer and knock-on collision mechanisms is studied with the code LUKE, a solver of the 3D (one spatial and two momentum dimensions) linearized bounce-averaged relativistic electron Fokker–Planck equation [2]. The code LUKE handles arbitrary shapes of the flux surfaces, but in this work the magnetic flux surfaces are assumed to remain circular and concentric as in the Tore Supra tokamak. They are assumed to remain intact throughout the runaway formation process, an assumption that would be too restrictive for the thermal quench in disruptive scenarios.

Modelling the evolution of the temperature and electric field in disruptions would require a proper description of the thermal quench including radiative or convective loss mechanisms and MHD instabilities. The coupling of a kinetic code capable of handling 3D magnetic topologies and open field lines with a fluid code such as JOREK [14] would be necessary for such a purpose, but is beyond the scope of this work. The kinetic modelling of the formation of runaway electrons is therefore done for non-disruptive scenarios as found in the current flattop with constant electric field and plasma temperature. With the restrictions of disruption modelling in mind, the objective of this work is to study the formation of runaway electrons in non-disruptive scenarios owing to the combined effect of Dreicer and knock-on collisions with a fast solver for the electron distribution function, in order to make predictions for the birth of runaway electrons in tokamak experiments.

The LUKE code has previously been used for current drive and Dreicer runaway calculations. The model uses a relativistic collision operator for small angle collisions and a recently added description of the large angle (knock-on) collisions leading to the avalanche effect, which enables a description of the full 2D momentum dynamics of the runaway population. Runaway electrons generated via knock-on collisions are typically scattered off with a significant perpendicular component of the momentum with respect to the local magnetic field direction. In a non-uniform magnetic field configuration, highly magnetized electrons could be subject to magnetic trapping effects resulting in reduced runaway electron growth rate off the magnetic axis in comparison to estimates obtained for a cylindric geometry. Such toroidicity effects are studied by implementing a 2D kinetic description of the knock-on momentum dynamics, including the momentum dynamics both perpendicular and parallel to the magnetic field lines.

Knock-on collisions are included in the kinetic equation through a source term from [3], implemented along with a sink term to ensure a particle conserving form of the process. The bounce-averaged knock-on source term is presented in section 2. In section 3 the effect of magnetic field non-uniformity is investigated. The role played by the magnetic mirror force on the runaway population off the magnetic axis, owing to a reduction in Dreicer growth rate as well as the high magnetization of the knock-on electrons, is described. Finally, in section 4, the relative importance of the avalanche effect compared to the Dreicer mechanism is quantified as

a function of plasma temperature and toroidal electric field strength. The parametric dependencies of the relative importance of the avalanche effect obtained from the numerical modelling are related to both analytic predictions and experimental data from runaway observations in non-disruptive scenarios from several tokamaks. The comparison includes a low density flattop pulse from the Tore Supra tokamak, during which suprathermal electrons are observed. The analysis of this scenario supports recently published results [13], showing that runaway electron formation requires lower density than expected from collisional theory, which suggests the existence of additional runaway electron loss mechanisms.

2. Knock-on collisions model

A knock-on collision between an existing runaway electron and a slower electron is considered. This paper follows the model from [3] in which the target electron is assumed to be at rest whereas the initial runaway travels at the speed of light in the direction of the magnetic field. This approximation will be justified later in this section. The target electron gains a momentum p from the close collision. As both energy and momentum must be conserved in the collision process, the secondary electron is scattered with a pitch-angle with respect to the direction of the incoming electron, which cosine ξ^* is given by the relation

$$\xi^* = \sqrt{\frac{\gamma - 1}{\gamma + 1}}, \tag{2}$$

where $\gamma = \sqrt{1 + p^2}$ is the relativistic factor and the momentum p is normalized to $m_0 c$.

The relativistic electron electron differential cross section derived by Møller [15] yields

$$\frac{\mathrm{d}\sigma}{\mathrm{d}\Omega} = r_e^2 \frac{1}{p\gamma(\gamma - 1)^2} \delta(\xi - \xi^*(p)), \tag{3}$$

where $r_e = e^2/(4\pi\varepsilon_0 m_e c^2)$ is the classical electron radius. As $\mathrm{d}\sigma/\mathrm{d}\Omega$ decrease rapidly with momentum, a large fraction of secondary electrons have a moderate kinetic energy with $\gamma - 1 \ll 1$ and are thus scattered with a large pitch-angle characterized by $\xi^* \ll 1$. Hence it is necessary to properly account for the 2D guiding-center momentum dynamics in non-uniform magnetic field geometries, where the electrons are influenced by the magnetic trapping effect.

The source term originally formulated in [3] is proportional to both the target population, i.e. the bulk electron density n_e and the existing runaway electron population n_r

$$\begin{aligned} \mathbf{S}(\psi, p, \xi) &= n_e(\psi) n_r(\psi) c \frac{\mathrm{d}\sigma}{\mathrm{d}\Omega}(p, \xi) \\ &= \frac{n_r}{4\pi\tau \ln\Lambda} \frac{1}{p^2} \frac{\mathrm{d}}{\mathrm{d}p} \left[\frac{1}{1 - \sqrt{1 + p^2}} \right] \delta(\xi - \xi^*(p)), \end{aligned} \tag{4}$$

where ψ is the poloidal magnetic flux surface coordinate. In the expression above, the collision time for relativistic electrons

$$\tau = \frac{4\pi\varepsilon_0^2 m_e^2 c^3}{n_e e^4 \ln\Lambda}, \tag{5}$$

has been introduced.

An analytic estimate of the avalanche growth rate is obtained from integration of the knock-on source term in equation (4) over the runaway region $p > p_c$ in momentum space, as done in the work by Rosenbluth, which yields the following expression for $E > E_c$ [3]

$$\frac{1}{n_r} \frac{\partial n_r}{\partial t} = \frac{1}{2\tau \ln\Lambda} \left(\frac{E}{E_c} - 1 \right). \tag{6}$$

2.1. Implementation of knock-on collisions in the LUKE code

The Rosenbluth model (equation (4)) for the runaway generation through knock-on collisions is implemented in the code LUKE. Electrons with a momentum larger than $p_{re} \equiv \max[p_c; p(E_k = 1\ \mathrm{MeV})]$ are accounted for in the population n_r of primary runaways for the knock-on collision process. The numerical momentum grid boundary p_{max} must be chosen to be larger or equal to p_{re} and electrons leaving the domain through the boundary remain accounted for in n_r.

To be valid, the Rosenbluth approximation requires that: (a) primary runaways in the knock-on collision process have a velocity near the speed of light, and (b) primary electrons have a momentum much larger than target electrons. The condition (a) is ensured by the 1 MeV minimum condition in p_{re}, which corresponds to $v/c \geqslant 0.94$, whereas the condition (b) is guaranteed by restricting the model to plasmas with $T_e \ll 1$ MeV. The Rosenbluth approximation is further justified by the weak dependence of the knock-on source term upon the incident electron energy in the energy range 1–100 MeV [16].

The bulk electron density is defined as the integral of the bulk electron distribution in momentum space:

$$\int_0^{p_{re}} f(r, p) \mathrm{d}^3 p = n_e(r). \tag{7}$$

The bulk and the runaway region, corresponding to $p < p_{re}$ and $p > p_{re}$ respectively, are shown in figure 1. The runaway electron population is the integral over both Dreicer and knock-on runaway fluxes

$$n_r(t) = \int_0^t \left(\gamma_D + \int_{p_{re}}^{p_{max}} S\ \mathrm{d}^3 p \right) \mathrm{d}t,$$

where $\gamma_D = \iint \mathbf{S_p}(\psi, p, \xi) \cdot \mathrm{d}\mathbf{S}$ is the integral of the particle flux through the surface $p = p_{re}$. In order to ensure conservation of number of particles in LUKE, a sink term is implemented to compensate for the knock-on source term

$$\mathbf{S} = \mathbf{S}_+ - < \mathbf{S}_+ > \frac{f_M}{< f_M >}, \tag{8}$$

where f_M is the bulk distribution, assumed to be Maxwellian and $< ... >= \int_0^{p_{max}} ... \mathrm{d}^3 p$. The source and sink terms ensure that the number of electrons $n_e + n_r = n_{tot}$ is conserved.

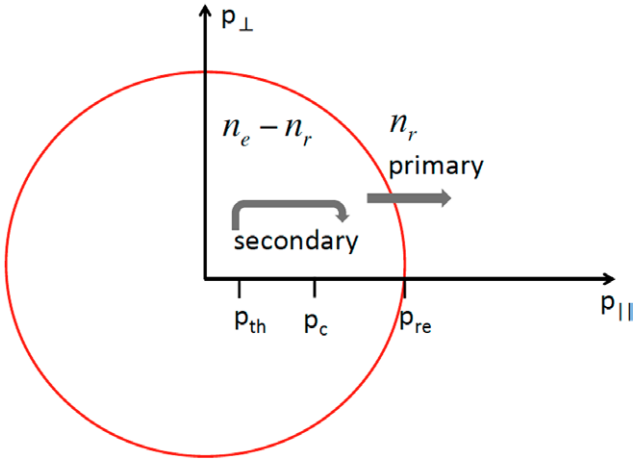

Figure 1. The LUKE momentum space is divided into two separate populations: the bulk electrons with momentum $p < p_{re}$ and the runaway electrons $p > p_{re}$. The knock-on collisions between the populations n_r and n_e can lead to secondary runaway electrons. Electrons that escape the domain $p < p_{re}$ by diffusion through p_{re} contribute to the runaway electron population n_r.

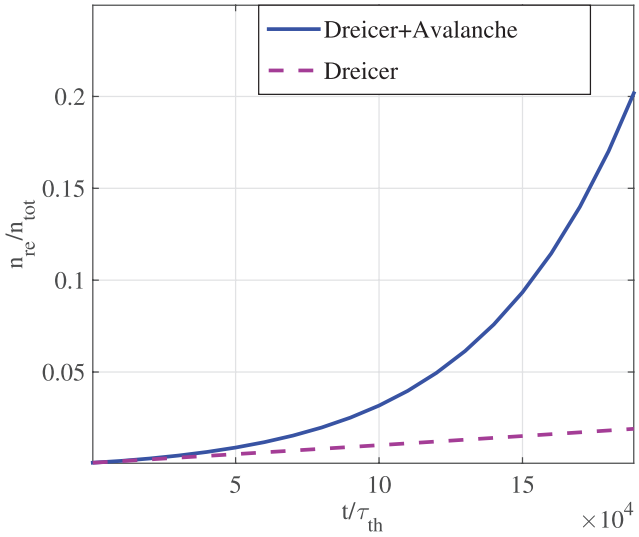

Figure 2. The fraction of runaway electrons ($E/E_c = 30$, $T_e = 0.5$ keV and $n_{tot} = 2 \cdot 10^{19}$ m^{-3}) as a function of time normalized to thermal collision time (here $\tau_{th} \approx 3.5 \cdot 10^{-6}$ s), with and without the avalanche effect due to the knock-on collisions.

2.2. Runaway electron growth rate

The runaway electron dynamics implemented in LUKE captures the combined effect of Dreicer and knock-on processes. The evolution of the runaway electron population under the influence of a constant electric field is calculated. Figure 2 shows the evolution of a runaway electron fraction with and without knock-on collisions. At first, there are very few runaway electrons, the knock-on contribution becomes significant only when a primary runaway electron population has been built up by the Dreicer effect. Then, an exponential growth of the runaway electron population is observed—describing the avalanche effect—and quickly becomes dominant over the Dreicer generation.

The avalanche mechanism is proportional to the bulk density $n_e = n_{tot} - n_r$, such that the runaway production rate can be expressed in the generic form

$$\frac{\partial n_r}{\partial t} = n_e(\gamma_D + \gamma_A) \rightarrow \frac{1}{(n_{tot} - n_r)} \frac{\partial n_r}{\partial t} = \gamma_D + \gamma_A. \quad (9)$$

To quantify the avalanche growth rate, the avalanche term may be expressed as $\gamma_A = n_r \bar{\gamma}_A$, where $\bar{\gamma}_A$ is an avalanche multiplication factor. Thus, equation (9) becomes:

$$\frac{1}{(n_{tot} - n_r)} \frac{\partial n_r}{\partial t} = \gamma_D + n_r \bar{\gamma}_A. \quad (10)$$

Equation (10) is an affine function of $n_r(t)$, where the constant term is the Dreicer growth rate and the avalanche multiplication factor is given by the slope. In figure 3 the growth rate given by equation (9) is illustrated for $E/E_c = 60$, $T_e = 0.5$ keV and $n_e = 2 \cdot 10^{19}$ m^{-3}. The growth rates from the LUKE calculations are evaluated numerically, the Dreicer as a constant value (γ_D) and the avalanche multiplication factor ($\bar{\gamma}_A$) from the slope of the curve. The Dreicer growth rate calculated by LUKE agrees well with predictions from Kulsrud [17] where the Fokker–Planck equation is solved numerically. The avalanche multiplication factor $\bar{\gamma}_A$ characterizes the tendency of a runaway avalanche to develop, for a given magnetic equilibrium and parallel electric field. The actual runaway production due to avalanche is however time dependent since it is a product of the avalanche multiplication factor $\bar{\gamma}_A$ and the time dependent runaway electron density n_r. For example, $\bar{\gamma}_A$ can be non-zero, even though the number of runaway electrons born from knock-on collisions is negligible until a seed of primary electrons is established.

For the sake of simplicity, the Rosenbluth model in [3] considers only secondary electrons born with a momentum larger than p_c. However, electrons accelerated via a knock-on collision to an intermediate momentum $p_{th} < p < p_c$ could contribute to the runaway growth rate indirectly by populating the suprathermal region and thereby modifying the Dreicer flux. Numerically, three thresholds must be defined when implementing the Rosenbluth model (4): the minimum and maximum values for the secondary electron momentum, and the minimum value p_{re} above which runaways are counted as primary electrons in the knock-on process. In order to determine these parameters, the lower threshold above which knock-on collisions are included is varied and the results are shown in figure 4 for electric field $E/E_c = 2$ and $E/E_c = 5$ ($T_e = 5$ keV). We can see that the indirect contribution of knock-on collisions to suprathermal energies $p_{th} < p < p_c$ is negligible, such that it is appropriate to set the lower threshold for secondary electron momentum at p_c. Energy conservation imposes that the higher threshold for secondary electron momentum is lower than p_{re}. We see that setting $p_{re} = 4p_c$ is sufficient to account for more than 80% of knock-on collisions while ensuring energy conservation.

2.3. Bounce-averaged knock-on source term

Since knock-on accelerated electrons emerge with high perpendicular momentum [3], it is necessary to properly account for the guiding-center dynamics in non-uniform magnetic

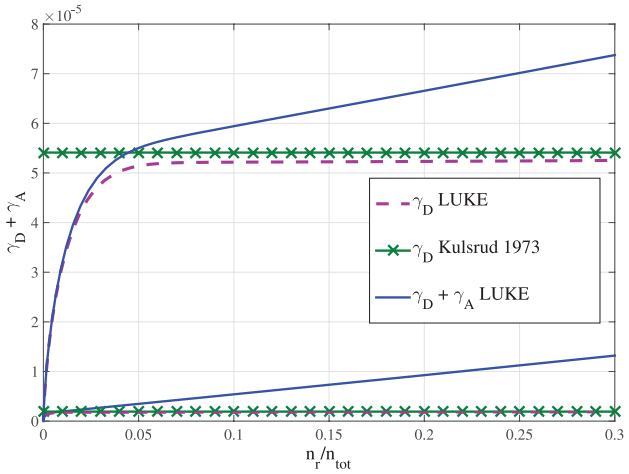

Figure 3. The growth rate in constant electric field in $T_e = 0.5$ keV and $n_{tot} = 2 \cdot 10^{19}$ m^{-3} for $E/E_c = 60$ i.e. $E/E_D = 0.06$ as a function of the runaway electron density, with and without the avalanche effect. For $n_r/n_{tot} < 0.05$ ($t \lesssim 2400\tau_{th} \approx 8$ ms) the growth rate has yet to reach its asymptotic value. The Dreicer contribution is in good agreement with Kulsrud's theory in the asymptotic limit [17]. The growth rates are normalized to the thermal collision frequency ($\nu_{th} = 1/\tau(v_{th}) \approx 2.9 \cdot 10^5$ s^{-1}).

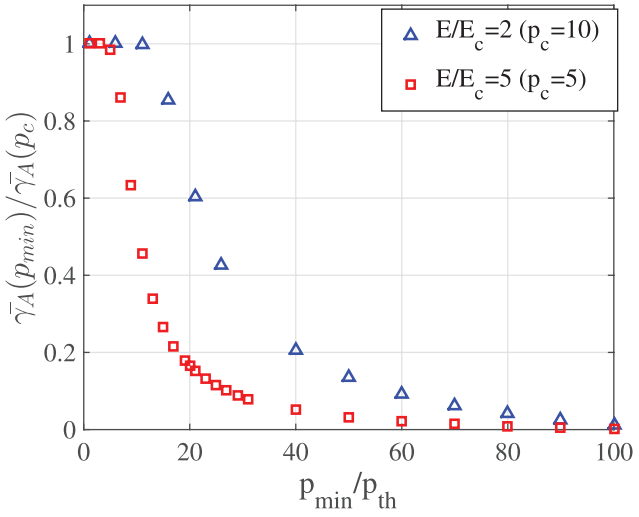

Figure 4. Avalanche multiplication factor as a function of the lower momentum cut off p_{min}/p_{th} for $T_e = 5$ keV, normalized to the avalanche factor at $p_{min} = p_c$.

field geometry and treat the full 2D momentum electron dynamics. In a non-uniform magnetic field, the magnetic moment is an adiabatic invariant such that the guiding center parallel velocity varies along the electron trajectory. The pitch angle coordinate ξ in equation (4) can be expressed as a function of (ξ_0, ψ, θ) where ξ_0 is the pitch angle measured at the poloidal position θ_0 of the minimum magnetic field $B_0(\psi)$ on a magnetic flux surface. When the collisional time is longer than the bounce period [2], the rapid poloidal motion ensures that the electron distribution $f(\psi, p, \xi_0)$ is independent of the poloidal angle θ. The poloidal angle dependence can thus be averaged out of the kinetic equation by bounce-averaging, defined as

$$\{\mathbf{S}\}(\psi, p, \xi_0) = \frac{1}{\lambda\tilde{q}}\left[\frac{1}{2}\sum_{\sigma}\right]_T \int_{\theta_{min}}^{\theta_{max}} \frac{d\theta}{2\pi}\frac{1}{|\hat{\psi}\cdot\hat{r}|}\frac{r}{R_p}\frac{B}{B_p}\frac{\xi_0}{\xi}\mathbf{S}(\psi, p, \xi), \tag{11}$$

where R_p is the major radius, θ_{min} and θ_{max} are the poloidal turning points for the trapped electrons, B_p is the poloidal component of the magnetic field B and the sum over σ applies to trapped particles (T) only. The normalized bounce time is

$$\lambda(\psi) = \frac{1}{\tilde{q}(\psi)}\int_{\theta_{min}}^{\theta_{max}} \frac{d\theta}{2\pi}\frac{1}{|\hat{\psi}\cdot\hat{r}|}\frac{r}{R_p}\frac{\xi_0}{\xi}\frac{B}{B_p}, \tag{12}$$

with

$$\tilde{q}(\psi) \equiv \int_0^{2\pi} \frac{d\theta}{2\pi}\frac{1}{|\hat{\psi}\cdot\hat{r}|}\frac{r}{R_p}\frac{B}{B_p}. \tag{13}$$

In the code LUKE, the electron distribution is normalized to a reference density $n_e^\dagger$ and the time evolution is normalized to the reference thermal collision frequency $\nu_{coll}^\dagger = 1/\tau(v_{th})$, so that the resulting source term is $\bar{\mathbf{S}} = \mathbf{S}/\mathbf{S}^\dagger$ where $\mathbf{S}$ is from equation (4) and $\mathbf{S}^\dagger = n_e^\dagger \nu_{coll}^\dagger$ Momentum is normalized to the thermal momentum $\bar{p} = p/p_{th}$. The knock-on source term is decomposed as $\bar{\mathbf{S}}(\mathrm{p}, \psi, \xi, \theta) = \bar{\mathbf{S}}^* \delta(\xi - \xi^*(\bar{\mathrm{p}}))$ where

$$\bar{\mathbf{S}}^* = \frac{1}{4\pi}\frac{\beta_{th}^{\dagger 2}}{\ln\Lambda^\dagger}\bar{n}_e\bar{n}_r\frac{1}{\bar{p}\gamma(\gamma-1)^2}, \tag{14}$$

is independent of θ, so that $\{\bar{\mathbf{S}}\} = \bar{\mathbf{S}}^*\{\delta(\xi - \xi^*(\bar{p}))\}$, where $\beta_{th}^\dagger = v_{th}^\dagger/c$ and ξ is the pitch angle cosine at the poloidal angle position θ

$$\xi(\xi_0, \psi, \theta) = \sigma\sqrt{1 - \Psi(\psi, \theta)(1 - \xi_0^2)}. \tag{15}$$

Here $\Psi(\psi, \theta) = B(\psi, \theta)/B_0(\psi)$ and $\sigma = \mathrm{sign}(v_\parallel) = \mathrm{sign}(\xi_0)$ indicates the direction of the electrons along the magnetic field line. Using the general relation for Dirac's delta function $\delta(g(x)) = \sum_k \delta(x - x_k)/|g'(x_k)|$ where x_k are the zeros of the function $g(x)$ and $g'(x) = dg/dx$ provided that $g(x)$ is a continuously differentiable function and $g'(x)$ is non-zero:

$$\delta(\xi - \xi^*) = \sum_k \frac{2\delta(\theta - \theta_k^*)|\xi^*|}{|\Psi'(\psi, \theta_k^*)|(1 - \xi_0^2)}, \tag{16}$$

where θ_k^* is the poloidal angle at which the secondary electron emerges. From equation (15) θ_k^* is given by

$$\sigma\sqrt{1 - \Psi(\psi, \theta_k^*)(1 - \xi_0^2)} - \xi^* = 0, \tag{17}$$

or

$$\Psi(\psi, \theta_k^*) = \frac{B_{\theta_k^*}}{B_0} = \frac{1 - \xi^{*2}}{1 - \xi_0^2} = \frac{2}{(1 - \xi_0^2)(\gamma + 1)}. \tag{18}$$

Using equation (16), the delta function can be expressed as

$$\{\delta(\xi - \xi^*)\} = \frac{1}{\lambda\tilde{q}}\frac{1}{\pi}\sum_k \frac{1}{|\hat{\psi}\cdot\hat{r}|_{\theta_k^*}}\frac{r_{\theta_k^*}}{R_p}\frac{B_{\theta_k^*}}{B_{p,\theta_k^*}}\frac{\xi_0}{\xi_{\theta_k^*}} \frac{|\xi^*|}{|\Psi'(\psi, \theta_k^*)|(1 - \xi_0^2)}.$$

and since $B_{\theta_k^*} = (1-\xi^{*2})/(1-\xi_0^2)B_0$ with $\xi_{\theta_k^*} = \xi^*$

$$\{\delta(\xi-\xi^*)\} = \frac{1}{\lambda\tilde{q}}\frac{1}{\pi}\sum_k \frac{1}{|\hat{\psi}\cdot\hat{r}|_{\theta_k^*}}\frac{r_{\theta_k^*}}{R_p}\frac{B_0}{B_{p,\theta_k^*}}|\xi_0| \times \frac{(1-\xi^{*2})}{|\Psi'(\psi,\theta_k^*)|(1-\xi_0^2)^2}, \tag{19}$$

and the normalized, bounce-averaged avalanche operator becomes

$$\{\bar{\mathbf{S}}(p,\psi,\xi_0)\} = \frac{1}{2\pi^2}\frac{1}{\ln\Lambda^\dagger R_p}\bar{n}_e\bar{n}_r \times \frac{1}{\bar{p}^3\gamma(\gamma-1)}\frac{B_0}{\lambda\tilde{q}}\frac{|\xi_0|}{(1-\xi_0^2)^2}\sum_k\left[\frac{1}{|\hat{\psi}\cdot\hat{r}|}\frac{r}{B_p}\frac{1}{|\Psi'|}\right]_{\theta_k^*}, \tag{20}$$

using the relation $p^2 = (\gamma^2-1) = (\gamma-1)(\gamma+1)$ and $p = \bar{p}\beta_{\text{th}}$.

3. Effect of toroidicity

The reduction of the Dreicer runaway rate away from the magnetic axis has been identified in previous work [18] including with the code LUKE, which solves the bounce-averaged kinetic equation [2]. The poloidal dependence of the electric field is accounted for and the input value is the flux-surface averaged elecric field. At least three effects contribute to reduce the growth rate: the overall effect of the electric field on trapped electrons cancels out over one bounce period; the acceleration of passing electrons is also reduced as their pitch angle increases towards the high field side; the existence of a magnetic trapping cone creates larger pitch-angle gradients in the circulating region, thereby increasing the effect of pitch-angle scattering.

As discussed in section 2, secondary electrons emerging from the knock-on collisions are typically highly magnetized. Since the trapping effect increases off the magnetic axis in a non-uniform magnetic field configuration, the further away from the magnetic axis the electrons appear, the more they tend to be born trapped [3].

To quantify the tendency of magnetic trapping, the evolution of the runaway population is calculated in a scenario with circular plasma cross section and magnetic non-uniformity, with the inverse aspect ratio ranging from $\epsilon = 0$ to $\epsilon = a/R = 1$. The inverse aspect ratio of the Tore Supra tokamak is $\epsilon \approx 0.3$. The calculations in figure 5 reveal that the runaway electron population grows significantly slower off the magnetic axis than in the center.

In order to study the trapping effects on the runaway population, the Dreicer growth rate γ_D and the avalanche multiplication factor $\bar{\gamma}_A$ are calculated with the bounce-averaged code LUKE and quantified separately. The Dreicer growth rate is found to be strongly affected by the non-uniformity of the magnetic field, as shown in figure 6. A fit of the numerical results gives an analytic expression of the Dreicer growth rate $\gamma_{D}/\gamma_{D,\text{cyl}} = 1-\sqrt{2\epsilon/(1+\epsilon)}$. The results indicate that

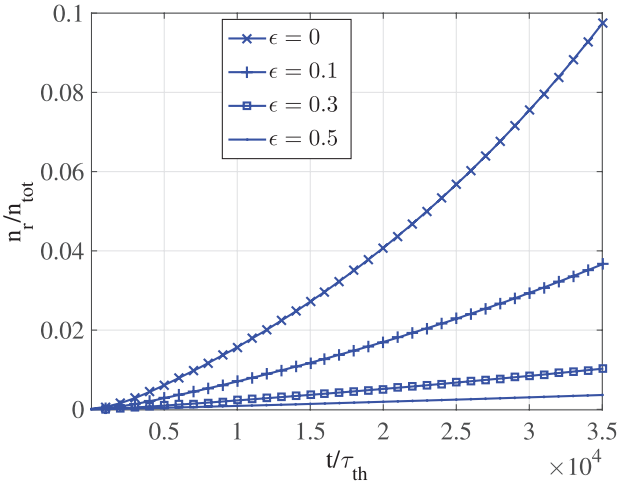

Figure 5. The evolution of the runaway electron population, including the avalanche effect owing to knock-on collisions, depends strongly on the radial position in a non-uniform magnetic field configuration, where $\epsilon = r/R$ is the inverse aspect ratio coordinate. $E/E_c = 40$, $T_e = 0.5$ keV, $n_e = 2\cdot 10^{19}$ m^{-3} and the time t is normalized to the thermal collision time $\tau_{th} \approx 3.5\cdot 10^{-6}$ *s*.

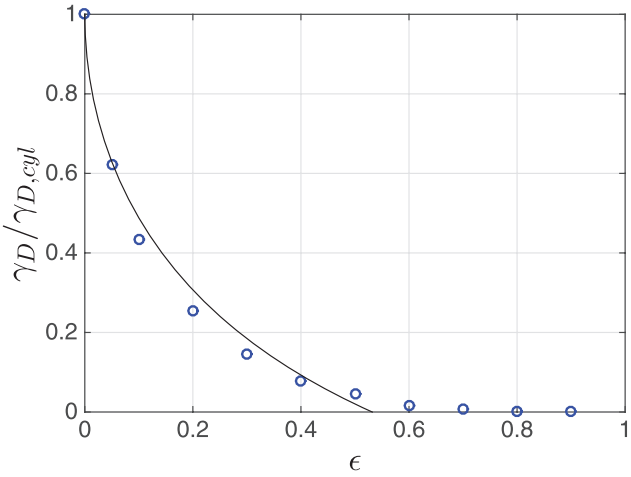

Figure 6. Radial dependence of Dreicer growth rate, normalized to the growth rate for cylindrical case $\epsilon = 0$ and a fit $\gamma_D/\gamma_{D,\text{cyl}} = 1 - 1.2\sqrt{2\epsilon/(1+\epsilon)}$.

for $\epsilon > 0.5$ runaway generation from Dreicer acceleration vanishes.

A reduction of $\bar{\gamma}_A$ away from the magnetic axis is observed in figure 7, with an avalanche multiplication factor that decreases with the inverse aspect ratio. In order to derive an analytical estimate for the avalanche growth rate including the effect of magnetic trapping owing to a non uniform magnetic configuration, it is assumed that all electrons with momentum $p > p_c$ will contribute to the runaway population (as in [3]), except the secondary electrons that appear in the trapped momentum region $p < p_T$. The magnetic trapping criterion on the momentum p_T of secondary electrons born via knock on collisions is

$$\frac{B(\theta)}{B_{\max}} > \frac{2}{\sqrt{1+p_T^2}+1}, \tag{21}$$

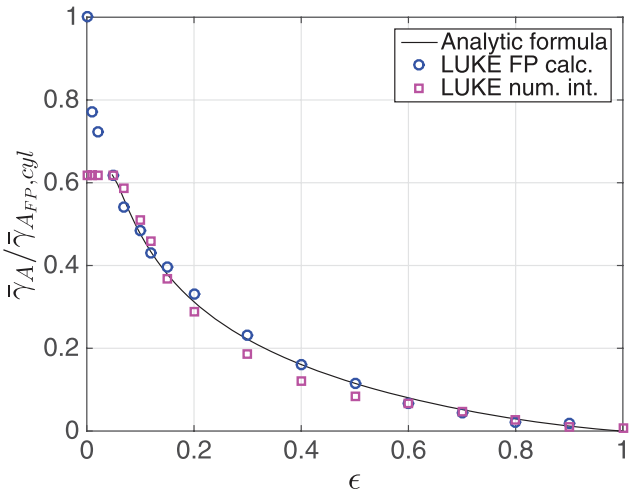

Figure 7. Radial dependence of the avalanche multiplication factor from bounce-averaged LUKE calculations (circles), normalized to to the avalanche multiplication factor for the cylindrical case $\epsilon = 0$. The numerical integration over the knock-on source term in equation (4) with the toroidal dependence in the momentum integration boundary is plotted in squares. The solid line shows the analytic estimate of the growth rate off the magnetic axis from equation (A.4).

where $B_{max}/B(\theta) = (1 + \epsilon\ \cos\ \theta)/(1 - \epsilon)$ in a circular concentric magnetic configuration. Electrons will run away if their momentum exceeds both the critical momentum and the trapping condition in equation (21). The lower integration limit p_{min} for the analytical estimate of the avalanche growth rate is thus given by $\max(p_c, p_T)$. An analytical expression for the inverse aspect ratio dependent avalanche growth rate is obtained by integrating the source term from over momentum space from p_{min} to $p_{max} = \infty$, which results in a locally modified, inverse aspect ratio dependent avalanche growth rate

$$\begin{aligned}\frac{\mathrm{d}n_r}{\mathrm{d}t_n}(\theta,\epsilon) &= \frac{1}{2}\frac{1}{\ln\ \Lambda^\dagger}\bar{n}_e\bar{n}_r\frac{1}{\sqrt{1+p_{min}^2}-1}\\ &= \frac{1}{2}\frac{1}{\ln\ \Lambda^\dagger}\bar{n}_e\bar{n}_r\ \min\left(\frac{E}{E_c},\frac{(1-\epsilon)^2}{2\epsilon(1+\cos\theta)}\right).\end{aligned} \tag{22}$$

The flux surface averaged growth rate is derived in appendix A. For $\epsilon E/E_c \gg 1$, $\theta_b \to \pi$, the growth rate is reduced by a factor $(1-\epsilon)^2/\left(\pi\sqrt{\epsilon E/E_c}\right)$. The inverse aspect ratio dependence of the estimated avalanche growth rate obtained from equation (22) is compared to numerical results. In addition, a numerical integration of the source term is also performed, with the same criterion on the lower integration boundary in momentum space p_{min} as the analytic estimate in equation (A.4). The analytic result is also compared to avalanche growth rate from Fokker–Planck calculations with the LUKE code. In that case, the trapping conditions are the same as in the analytic result, except for that the critical momentum is pitch angle dependent $p_c^2 = E_c/(E\xi)$. The LUKE calculated avalanche multiplication factor and the analytical estimate show good agreement (figure 7).

Figure 7 shows the reduced growth rate for $E/E_c = 5$, relative to a cylindric plasma, equivalent to the growth rate on the magnetic axis ($\epsilon = 0$). Numerical integration of the source term shows good agreement with the analytic result (equation (A.4)). Close to the center, at low inverse aspect ratio, the effect of trapping is not visible, since the critical momentum is higher than the trapped momentum over the whole flux surface. This effect decreases with increasing E/E_c as the critical momentum p_c decreases and becomes less restrictive compared to the trapping condition p_T, which explains the flat top seen in figure 7. However, for the FP calculations the magnetic trapping effect influences the growth rate also close to the magnetic axis. A possible explanation is pitch angle collisions that couple the dynamics between the trapped and the passing region.

The growth rate obtained from bounce-averaged calculations suggest that the formation of runaway electrons is slower the further away from the magnetic axis they appear. In other words, the time scale of the local growth rate could be longer than suggested by collisional theory [3, 17]. Potential loss mechanisms, such as transport of fast electrons due to magnetic field perturbations [19] could therefore act more efficiently on the runaway electrons formed off the magnetic axis than the ones formed on axis which could lead to well confined runaway electrons at the center of the plasma.

4. The relative importance of the avalanche effect

The results presented in section 2.2 (see figure 2) have shown that the runaway electron distribution can be significantly modified by including the effect of knock-on collisions. In order to understand the mechanisms that govern the runaway electron generation processes a parametric study is performed with the aim to investigate which runaway formation process, Dreicer or avalanche, dominates in non-disruptive tokamak experiments.

The relative importance of the avalanche mechanism to the Dreicer mechanism can be estimated by comparing the analytic avalanche growth rate in equation (6) and the Dreicer generation that is derived in [6]:

$$\left(\frac{\partial n_r}{\partial t}\right)_D \sim \frac{2}{\sqrt{\pi}}n_e\nu(v_{th})\left(\frac{E}{E_D}\right)^{1/2}\exp\left(-\frac{E_D}{4E}-\left(\frac{2E_D}{E}\right)^{1/2}\right),$$

where $E_D = (c/v_{th})^2 E_c$ is the electric field at which even thermal electrons will run away, known as the Dreicer field. The ratio of the two growth rates is

$$\frac{\gamma_A}{\gamma_D} \sim \frac{\sqrt{\pi}}{4}\frac{n_r}{n_e}\frac{1}{\ln\Lambda}\left(\frac{v_{th}}{c}\right)^3\left(\frac{E}{E_c}-1\right)\left(\frac{E}{E_D}\right)^{-1/2}\exp\left(\frac{E_D}{4E}+\sqrt{\frac{2E_D}{E}}\right). \tag{23}$$

By letting a small fraction of electrons run away in LUKE, the relative importance of the avalanche effect as a function of plasma temperature and electric field strength can be evaluated numerically from the fraction of the runaway electrons that originate from Dreicer and knock-on collisions. In figure 8 the fraction of runaway electrons born from knock-on collisions is shown, when 1% of the initial electron population has run away in a cylindrical magnetic configuration with constant electric field, density and temperature. The fraction of

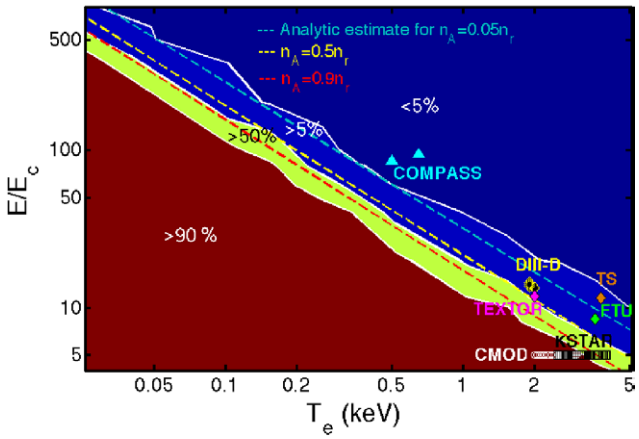

Figure 8. The fraction of runaways originating from knock-on collisions (n_A/n_r) as modelled in LUKE. The analytic estimate of when 5% (cyan line), 50% (yellow line) and 90% (red line) of the runaways come from avalanche is obtained from equation (23). Non-disruptive scenarios where runaway electrons were generated in several tokamaks are taken from [13] except for the Tore Supra (TS) point (discharge #40719) and COMPASS points (discharge #8555 and #8630).

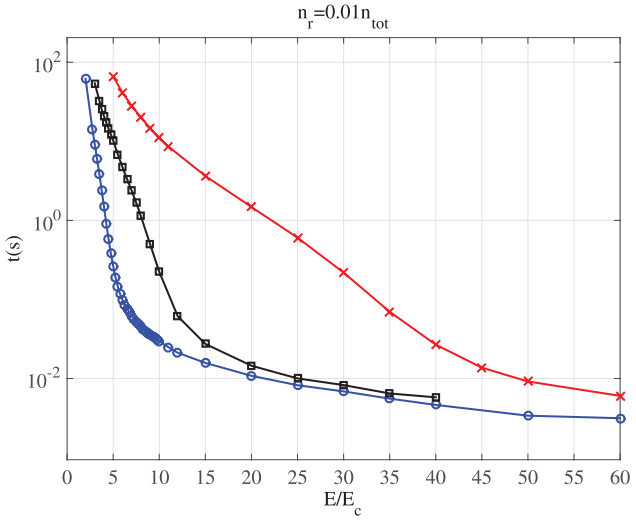

Figure 9. The time required for 1% of the Maxwellian electrons to run away, for the electron temperature $T_e = 0.5$ keV (dashed line), 2 keV (solid line and squares) and 5 keV (solid line and circles).

runaway electrons has to be small enough for the equilibrium parameters to remain constant. The relative importance of secondary runaway electrons grows at lower temperature and electric field, as the slower primary generation in high collisionality (low temperature) allows for runaway avalanches to take off. The time required to reach the runaway fraction varies strongly in the parameter space presented in figure 8. The time required for 1% of the electrons to run away is illustrated for various electron temperatures ($T_e = 0.05, 0.5, 2$ and 5 keV) in figure 9. The formation of runaway electrons slows down as the collisionality increases at lower bulk temperature.

The numerical results are compared with the analytical estimate from equation (23) with $n_r/n_e = 0.01$. The condition for the dominance of the avalanche effect $\gamma_A/\gamma_D > 1$ is plotted in figure 8 along with the boundaries for which $n_A/n_r = 5\%$ and 90%.

In order to relate the study to experimental tokamak scenarios, it must be noted that the simulations are performed for constant electric field and temperature. Consequently, the study is restricted to non-disruptive scenarios with well-diagnosed and quiescent conditions from several tokamaks, where runaway electrons have been observed in the current flattop with the relevant plasma parameters maintained essentially constant. Results from scenarios with reproducible measurements of electron density, loop voltage and plasma temperature at the runaway electron onset from DIII-D, FTU, TEXTOR, Alcator C-Mod and KSTAR were recently published in [13]. From this study the threshold electric field normalized to the critical field is found to be significantly higher than predicted by collisional theory where the birth of runaway electrons is predicted at $E/E_c > 1$, provided that no additional runaway electron loss mechanisms are present [17]. However, the condition for runaway onset in collisional theory does not take the time required to generate runaway electrons into account. Estimations from LUKE calculations in figure 9 shows that this time scale can be unrealistically large as compared to the tokamak discharge duration. The time to generate a small fraction of runaway electrons from a Maxwellian distribution is finite for $E/E_c > 1$ but as $E/E_c \to 1$, the required time to generate runaway electrons $t \to \infty$. However, it is not the only explanation since the study in [13] found that the E/E_c threshold for suppression is also well above unity.

Runaway electrons have been generated in the Tore Supra (TS) tokamak in low density discharges ($n_e < 10^{19}$ m^{-3}). The TS pulses #40719 and #40721 are performed after a boronization and suprathermal electrons are observed in the former discharge but not in the latter. Both are ohmic discharges at $I_p = 0.6$ MA in the current flattop. A possible signature of suprathermal electrons is observed in #40719 by the ECE edge chords at current ramp-up and ramp-down, when the density is low ($< n_e > = 0.4 \cdot 10^{19}$ m^{-3}), see figure 10(a). The uniform E-field, estimated as the time derivative of the resistive flux [20], is $E_\parallel = 0.038 \pm 0.003$ V m^{-1} and the core temperature is 3.8 keV. The determination of the magnetic flux at the plasma boundary is described in [21]. No suprathermal electrons are detected by electron cyclotron emission (ECE) in the following pulse #40721 at a higher electron density, see figure 10(b). Similar result is found from HXR measurements from the vertical camera detecting emission of 20–200 keV (figure 11). A peak of photo-neutrons is observed at the plasma termination for the lower density shot (#40719) but not for the higher density shot (#40721). It must be noted that the ECE signal alone is not a definite signature of runaway electrons, as its interpretation depends on the optical thickness of the plasma. However, it is from the combined observations on ECE, HXR and photo-neutron measurements, that the presence of relativistic electrons during the ramp-down of #40719 is identified. During the current flattop of #40719, the electron density is $< n_e > = 0.64 \cdot 10^{19}\ m^{-3}$, corresponding to $E/E_c \approx 8$ or $E/E_D \approx 0.06$, but there is no sign of suprathermals until $E/E_c \approx 11$. The suprathermal generation in #40719 is added to the $(E/E_c, T_e)$ scan (see figure 8) and lands in the region where Dreicer generation is dominant. In the higher density pulse

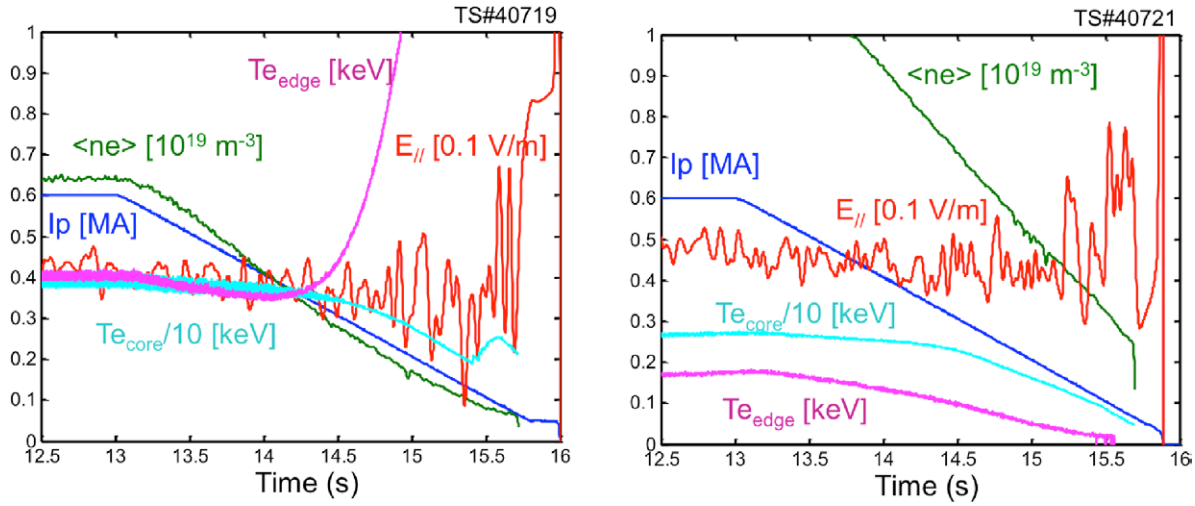

Figure 10. Possible signature of suprathermal electrons on the edge ECE chord ($T_{e,edge}$) at around $t = 14.5$ s are seen in the Tore Supra discharge 40719 (left). In a following discharge, with higher density (right), there is no sign of suprathermal electrons on the ECE measurements. E_l is the electric field strength, $<n_e>$is the line averaged density and l_p is the plasma current.

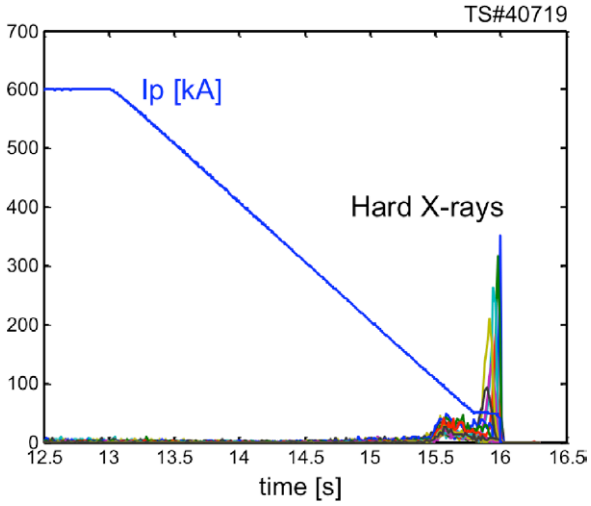

Figure 11. HXR data from the vertical camera (channels 1–21) in the energy range $E_{HXR} = 20$–200 keV. The HXR emission produced in the current ramp down in 40719 is a signature of suprathermal electrons, whereas in the higher density discharge 40721 no HXR emission is detected.

(#40721) $E/E_c \approx 4$ or $E/E_D = 0.02$ during the current flattop and no suprathermal electrons are detected. These results are in line with those of [13] where $E/E_c \sim 3$–12 is required to generate a detectable population of runaway electrons in the various tokamaks.

Relating the data from the experiments in [13] and the TS discharge #40719 to the parameter scan done in LUKE (figure 8) reveals that the scenarios fall in or close to the region where the avalanche mechanism becomes significant for the runaway electron growth rate (figure 8). Data from two COMPASS discharges where runaways were observed (#8555 and #8630) fall in the region where the Dreicer effect is dominant [22]. Runaway electrons are commonly produced in the current ramp-up phase of the COMPASS tokamak, due to the relatively high E/E_c ratio (20–200). The circular 130 kA discharge #8555 was part of the flattop line averaged electron density $< n_e >$ scan from 1–$4 \cdot 10^{19}$ m^{-3}, where $< n_e >$ for this particular shot was $2 \cdot 10^{19}$ m^{-3} during the flattop. The rise in runaway activity was observed with HXR NaI(Tl) scintillator and photoneutron detector as the $< n_e >$ decreased from discharge to discharge, while Parail–Pogutse instability appeared for all discharges with $< n_e >$ lower than in the discharge #8555. D-shaped 160 kA discharge #8630 was done for the purpose of the sawteeth-runaway correlation studies with the electron density $< n_e > = 9 \cdot 10^{19}$ m^{-3}. Even though the discharge had relatively high $< n_e >$, the runaway activity correlated with the sawteeth instability was visible in HXR and photoneutron signals. These two COMPASS discharges #8555 and #8630 are plotted on figure 8, where E/E_c at the ramp-up phase were 85 and 94, respectively. The electron density at the time of the runaway detection is $1.1 \cdot 10^{19}$ and $0.80 \cdot 10^{19}$ m^{-3}. In COMPASS, interferometry is used for the line averaged electron density $< n_e >$ measurements, while Thomson scattering is used for electron temperature T_e and electron density n_e profile measurements.

These observations suggest that knock-on collisions may contribute to the formation of runaway electron generation in tokamak plasmas, even in non-disruptive scenarios. The study predicts that avalanches can play an important role during current flattop. A self consistent electric field and equilibrium solver would be necessary to study avalanches with LUKE in disruptions, but is beyond the scope of the current work.

5. Conclusion

In this work the growth of runaway electron populations through the combined effect of Dreicer and knock-on collision mechanisms is studied. The Rosenbluth [3] model is extended to non-uniform magnetic field configurations and implemented as a bounce-averaged conservative source/sink term within the kinetic equation in the 3D Fokker–Planck solver LUKE. Dependencies of key parameters such as electric field

strength, electron temperature, and density are investigated. In addition, magnetic trapping effects are quantified in a non-uniform magnetic equilibrium, resulting in a reduced runaway population off the magnetic axis for both the Dreicer and the avalanche mechanism.

The kinetic modelling of the formation of runaway electrons is restricted to non-disruptive scenarios as found in the current flattop with non-transient electric field and plasma temperature. Modelling the rapidly varying temperature and electric field found in disruptions would require a proper description of the thermal quench with implemented radiative or convective loss mechanisms of the plasma energy, including MHD instabilities. The extension of the kinetic code LUKE to 3D magnetic configuration and its coupling with a fluid code such as JOREK [14] would be necessary for such a purpose and is beyond the scope of this work. In the present paper, runaways are confined to the flux-surface where they are generated, such that the growth rate derived herein should be considered as upper estimates.

Since knock-on accelerated electrons emerge with high perpendicular momentum, the full 2D guiding-center momentum dynamics is taken into account via a bounce-averaged description. The effect of magnetic trapping of the electrons in a non-uniform magnetic field configuration, known as the magnetic mirror effect, has been investigated, revealing reduction of both Dreicer and avalanche mechanisms off the magnetic axis. An analytical expression for avalanche growth rate accounting for magnetic trapping is derived. It is in agreement with numerical simulations and shows that a significant proportion of secondary electrons are knocked into the trapped region off the magnetic axis. The reduction of the off axis growth rate implies that the time scale of runaway formation is longer at the edge than close to the center, which means that potential loss mechanisms such as radial electron transport could compete with the acceleration of runaway electrons at the edge.

Moreover, quantifying the relative importance of avalanche generation as a function of plasma temperature and electric field strength, the simulations reveal that runaway electrons originating from knock-on collisions dominate at low temperature and electric field strength and likely play a significant role in runaway generation processes in several tokamaks with data from non-disruptive scenarios that are presented in [13]. The onset of runaway electrons found in these experiments is related to LUKE simulations of corresponding electric field and temperature in order to evaluate the importance of the avalanche effect, revealing that knock-on collisions may play a significant role also in non-disruptive scenarios. The LUKE calculations predict runaway electron generation also in a near critical field, in agreement with collisional theory if no other runaway electron loss mechanisms than collisional damping are present. However, the time to generate runaway electrons can be significantly greater compared to the duration of the phase in which $E/E_c > 1$ in experiments. In addition, the required time for runaway electron formation is very sensitive to the bulk electron temperature. The lack of runaway electron signatures near the critical electric field could therefore be explained by the long time scale required for their formation. To understand this discrepancy between observations and theory, the existence of additional loss mechanisms that dominate during the current flattop must be addressed. One possible candidate is transport of fast electrons due to magnetic field perturbations [19]. Once such additional runaway electron loss mechanisms have been identified, the LUKE code may form an excellent test bed for quantifying these effects, which will be the objective of future work.

Acknowledgments

This work has been carried out within the framework of the EUROfusion Consortium and has received funding from the Euratom research and training programme 2014-2018 under grant agreement No 633053. The views and opinions expressed herein do not necessarily reflect those of the European Commission.

Appendix A. Derivation of toroidicity dependent avalanche growth rate

As described in section 3, the avalanche growth rate is evaluated by the flux surface averaged knock-on source term in equation (4) where the lower integration boundary is set by the maximum of the critical momentum p_c and the momentum defining the boundary of a passing and a trapped electron p_T, given by the trapping condition in equation (21). For finite E/E_c, the critical momentum $p_c > 0$. As the growth rate is averaged over the poloidal angle, $p_{min} \to p_c$ as the high field side is approached ($p_T \to 0$ as $\theta \to \pi$). The growth rate becomes:

$$\frac{dn_r}{dt_n}(\theta,\epsilon) = \frac{1}{2}\frac{1}{\ln\Lambda}\bar{n}_e\bar{n}_r\frac{1}{\sqrt{1+p_{min}^2}-1} \tag{A.1}$$

$$= \frac{1}{2}\frac{1}{\ln\Lambda}\bar{n}_e\bar{n}_r \min\left(\frac{E}{E_c}, \frac{(1-\epsilon)^2}{2\epsilon(1+\cos\theta)}\right). \tag{A.2}$$

The poloidal angle θ_{bound} where $p_c = p_T$ constitutes the boundary between the region where the avalanche rate is limited either by the drag force or by the magnetic trapping effect. This angle is obtained from the condition $p_c = p_T$:

$$1+\cos\,\theta_{bound} = (1-\epsilon)^2/\left(2\epsilon\frac{E}{E_c}\right) \to$$

$$\theta_{bound} = \pm\arccos\left((1-\epsilon)^2/\left(2\epsilon\frac{E}{E_c}\right)-1\right).$$

If $\epsilon E/(E_c(1-\epsilon)^2) < 1/4$, p_c is the lower integration limit p_{min} and if $\epsilon E/(E_c(1-\epsilon)^2) > 1/4$, $p_{min} = p_T(\theta)$. Averaged over the flux surface according to volumic flux surface average the growth rate is:

$$< \frac{\mathrm{d}n_\mathrm{r}}{\mathrm{d}t_n} >_V (\epsilon) = \frac{1}{\hat{q}}\left(\frac{1}{\pi}\int_0^{\theta_\mathrm{bound}} \epsilon \frac{B_0(\epsilon)}{B_P}\frac{\mathrm{d}n_\mathrm{r}}{\mathrm{d}t_n}(p_\mathrm{T}(\theta))\mathrm{d}\theta + \frac{1}{\pi}\int_{\theta_\mathrm{bound}}^{\pi} \epsilon \frac{B_0(\epsilon)}{B_P}\frac{\mathrm{d}n_\mathrm{r}}{\mathrm{d}t_n}(p_\mathrm{c})\mathrm{d}\theta\right) = \frac{1}{2}\frac{1}{\ln\Lambda^\dagger}\bar{n}_\mathrm{e}\bar{n}_\mathrm{r} \times\left((1+\epsilon)\frac{B_p}{B}\frac{1}{\pi}\int_0^{\theta_\mathrm{bound}} \frac{B_0(\epsilon)}{B_P}\frac{(1-\epsilon)^2}{2\epsilon(1+\cos\theta)}\mathrm{d}\theta + (1+\epsilon)\frac{E}{E_\mathrm{c}}\frac{1}{\pi}\int_{\theta_\mathrm{bound}}^{\pi}\frac{(1+\epsilon\,\cos(\theta))}{1+\epsilon}\mathrm{d}\theta\right). \tag{A.3}$$

In the above calculation circular concentric flux surfaces are considered so that $|\hat{\psi}\cdot\hat{r}|= 1$, $r/R_p = \epsilon$ and

$$\hat{q} = \int_0^{2\pi}\frac{\mathrm{d}\theta}{2\pi}\epsilon\frac{B_0}{B_p} = \int_0^{2\pi}\frac{\mathrm{d}\theta}{2\pi}\epsilon\frac{(1+\epsilon\,\cos(\theta))}{(1+\epsilon)}\frac{B}{B_p} = \frac{\epsilon}{(1+\epsilon)}\frac{B}{B_p}.$$

The flux surface averaged growth rate takes the form:

$$< \frac{\mathrm{d}n_\mathrm{r}}{\mathrm{d}t_n} >_V(\epsilon) = \frac{1}{2\,\ln\Lambda^\dagger}\bar{n}_\mathrm{e}\bar{n}_\mathrm{r}\frac{E}{E_\mathrm{c}} \times\left(1-\frac{\theta_\mathrm{bound}}{\pi}-\frac{\epsilon}{\pi}\sin(\theta_\mathrm{bound})\right) + (1-\epsilon)^2\frac{1}{2\epsilon\pi}((1-\epsilon)\tan(\theta_\mathrm{bound}/2)+\epsilon\theta_\mathrm{bound}) = \frac{1}{2\,\ln\Lambda^\dagger}\bar{n}_\mathrm{e}\bar{n}_\mathrm{r}\frac{E}{E_\mathrm{c}} \times\left(1-\frac{\theta_\mathrm{bound}}{\pi}-\frac{\epsilon}{\pi}\sin(\theta_\mathrm{bound}) + \frac{(1-\epsilon)^2E_\mathrm{c}}{2\epsilon\pi E}\left(\sqrt{1-\epsilon}\,\sqrt{4\epsilon E/E_\mathrm{c}-(1-\epsilon)}+\epsilon\theta_\mathrm{bound}\right)\right), \tag{A.4}$$

where

$$\tan(\theta_\mathrm{bound}/2) = \frac{\sin(\theta_\mathrm{bound})}{1+\cos(\theta_\mathrm{bound})} = \frac{\sqrt{4\epsilon E/E_\mathrm{c}-(1-\epsilon)}}{\sqrt{1-\epsilon}}.$$

For $\epsilon E/E_\mathrm{c} \gg 1$, $\theta_b \to \pi$ and the growth rate is reduced by a factor $(1-\epsilon)^2/\left(\pi\sqrt{\epsilon E/E_\mathrm{c}}\right)$.

References

[1] Hender T C *et al* 2007 MHD stability, operational limits and disruptions *Nucl. Fusion* **47** S128–202

[2] Decker J and Peysson Y 2004 DKE: a fast numerical solver for the 3D drift kinetic equation *Report* EUR-CEA-FC-1736, Euratom-CEA

[3] Rosenbluth M N and Putvinski S V 1997 Theory for avalanche of runaway electrons in tokamaks *Nucl. Fusion* **37** 1355–62

[4] Wesson J A *et al* 1989 Disruptions in JET *Nucl. Fusion* **29** 641–66

[5] Tavani M *et al* 2011 Terrestrial gamma-ray flashes as powerful particle accelerators *Phys. Rev. Lett.* **106** 018501

[6] Connor J W and Hastie R J 1975 Relativistic limitations on runaway electrons *Nucl. Fusion* **15** 415–24

[7] Dreicer H 1959 Electron and ion runaway in a fully ionized gas. I *Phys. Rev.* **115** 238–49

[8] Lehnen M *et al* 2011 Disruption mitigation by massive gas injection in JET *Nucl. Fusion* **51** 123010

[9] Lehnen M *et al* 2009 Runaway generation during disruptions in JET and TEXTOR *J. Nucl. Mater.* **390–1** 740–6

[10] Hollmann E M *et al* 2015 Status of research toward the ITER disruption mitigation system *Phys. Plasmas* **22** 021802

[11] Nedospasov A V 2008 Thermal quench in tokamaks *Nucl. Fusion* **48** 032002

[12] Jaspers R, Finken K H, Mank G, Hoenen F, Boedo J A, Cardazo N J L and Schuller F C 1993 Experimental investigation of runaway electron generation in textor *Nucl. Fusion* **33** 1775

[13] Granetz R S, Esposito B, Kim J H, Koslowski R, Lehnen M, Martin-Solis J R, Paz-Soldan C, Rhee T, Wesley J C and Zeng L 2014 An ITPA joint experiment to study runaway electron generation and suppression *Phys. Plasmas* **21** 072506

[14] Huysmans G T A and Czarny O 2007 MHD stability in x-point geometry: simulation of ELMs *Nucl. Fusion* **47** 659–66

[15] Møller C 1932 *Ann. Phys.* **14** 531–85

[16] Chiu S C, Rosenbluth M N, Harvey R W and Chan V S 1998 Fokker-planck simulations of knock-on electron runaway avalanche and bursts in tokamaks *Nucl. Fusion* **38** 1711–21

[17] Kulsrud R M, Sun Y-C, Winsor N K and Fallon H A 1973 Runaway electrons in a plasma *Phys. Rev. Lett.* **31** 690–3

[18] Eriksson L G and Helander P 2003 Simulation of runaway electrons during tokamak disruptions *Comput. Phys. Commun.* **154** 175–96

[19] Zeng L *et al* 2013 Experimental observation of a magnetic-turbulence threshold for runaway-electron generation in the TEXTOR tokamak *Phys. Rev. Lett.* **110** 235003

[20] Ejima S, Callis R W, Luxon J L, Stambaugh R D, Taylor T S and Wesley J C 1982 Volt-second analysis and consumption in Doublet III plasmas *Nucl. Fusion* **22** 1313

[21] Wijnands T and Martin G 1997 An advanced plasma control system for Tore Supra *Fusion Technol.* **32** 471–86

[22] Vlainic M, Mlynar J, Cavalier J, Weinzettl V, Paprok R, Imrisek M, Ficker O, Noterdaeme J-M and the COMPASS Team 2015 Post-disruptive runaway electron beam in COMPASS tokamak *J. Plasma Phys.* Accepted